As a simple example of the application of numerical analysis, the problem of a vertically loaded surface footing resting on an undrained clay. To be consistent with conventional foundation design, the undrained clay is modelled using a linear elastic Tresca model. Results from this analysis are compared with the conventional bearing capacity solutions. The modes of bearing capacity failure are shown in Figure 1.

Analyses have been performed to obtain the load-displacement curves for rigid strip surface footings. The soil was assumed to be elasto-plastic with a Tresca yield surface and properties: $E = 8$MPa , $\mu = 0.49$ and $S_u = 100$kPa. The mesh shown in Figure 2 was used. The two vertical sides of the mesh have been restrained in the horizontal direction, while the base of the mesh was not allowed to move in either the vertical or horizontal direction. Loading was simulated by applying increments of vertical displacement to the soil surface below the position of the footing.

Table 1: Characteristic soil properties

Layer	Young's Modulus (kPa)	Poisson's Ratio	S_u (kPa)
Clay	8e+3	0.49	100

It is assumed from prior *experience* that the Young's modulus and the undrained shear strength of clay layers follow a normal distribution:

$$E \sim \mathcal{N}(\mu_1, \sigma_1^2)$$
$$S_u \sim \mathcal{N}(\mu_2, \sigma_2^2)$$

with

$$\mu_1 = 8.0E+3 \text{ kPa}, \qquad \sigma_1 = 3.0E+3 \text{ kPa}$$
$$\mu_2 = 100 \text{ kPa}, \qquad \sigma_2 = 20 \text{ kPa}$$

Forward Analysis

- Scatter plots of the prior sample distribution is given in Figure 3.
- A typical load displacement curve generated by the forward model is given in Figure 4.
- An experimental design of size 40 is first generated using the computational model ($\mathcal{M}$) for i.i.d. input parameters x. The range of outcomes for the experimental design is shown in Figure 5.

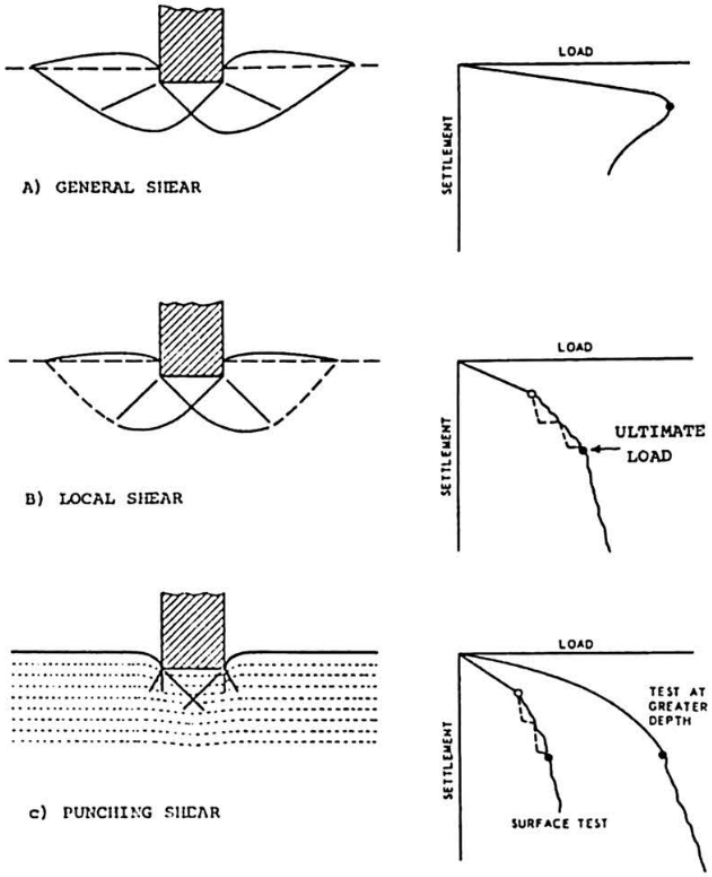

Figure 1: Stress increase in a layered soil system with a uniformly loaded circular area.

- We will treat this problem as a Markov Chain process.
- We will split the results into Stages 1, 2, 3 and 4. These stages correspond a center point displacement of 0.025, 0.05, 0.075 and 0.575m.
- From the 40 simulations, we are able to generate a PCE (surrogate) of the FE model for each of the loading stages.

Bayesian Inverse Analysis

- If we now run a Bayesian Inverse Analysis of the problem, we can infer the most appropriate set of input parameters for a given center point displacement.

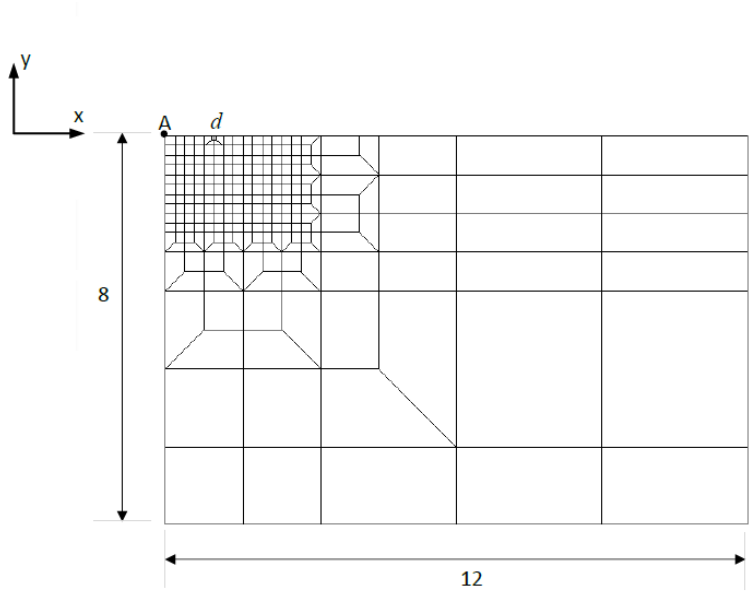

Figure 2: Axisymmetric finite element mesh of the loaded circular area problem.

- We measure 3 independent observations of the load at the end of each loading stages:
  $\mathcal{Y}_1 = \{144;\ 144;\ 145\}$ kN;
  $\mathcal{Y}_2 = \{279;\ 280;\ 280\}$ kN;
  $\mathcal{Y}_3 = \{367;\ 366;\ 366\}$ kN;
  $\mathcal{Y}_4 = \{551;\ 550;\ 551\}$ kN.

- To find the optimal set of values of the input parameters x we will first consider the input parameters as a random vector $X \sim \pi(x)$. The prior distribution will be informed by engineering experience (as described earlier). A plot of the prior distribution is given in Figure 3.

- The posterior distribution using the measured data at the end of each stage can be obtained by using Bayes Theorem. Given the observed data $\mathcal{Y}_1$, the posterior sample of input parameters x following the end of the first stage is plotted in Figure 6. The measured data and frequency histogram of the output is given in Figure 7.

- Results from the posterior distribution are used to update the prior distribution for the next stage. The process described in the above point is repeated to plot Figures 8 to 13

- The change in parameter distribution (E and s_u) with stage number is given in Figures 14 and 15. The model parameters used to obtain the observed load displacement curve ($\mathcal{Y}$) is given by the black dotted line.
- It is interesting to note that the convergence to the right solution is extremely rapid for the Young's modulus, only requiring the first stage to drastically reduce the variance. Undrained shear strength continued to improve. Variance for both parameters were found to decrease with stage number.

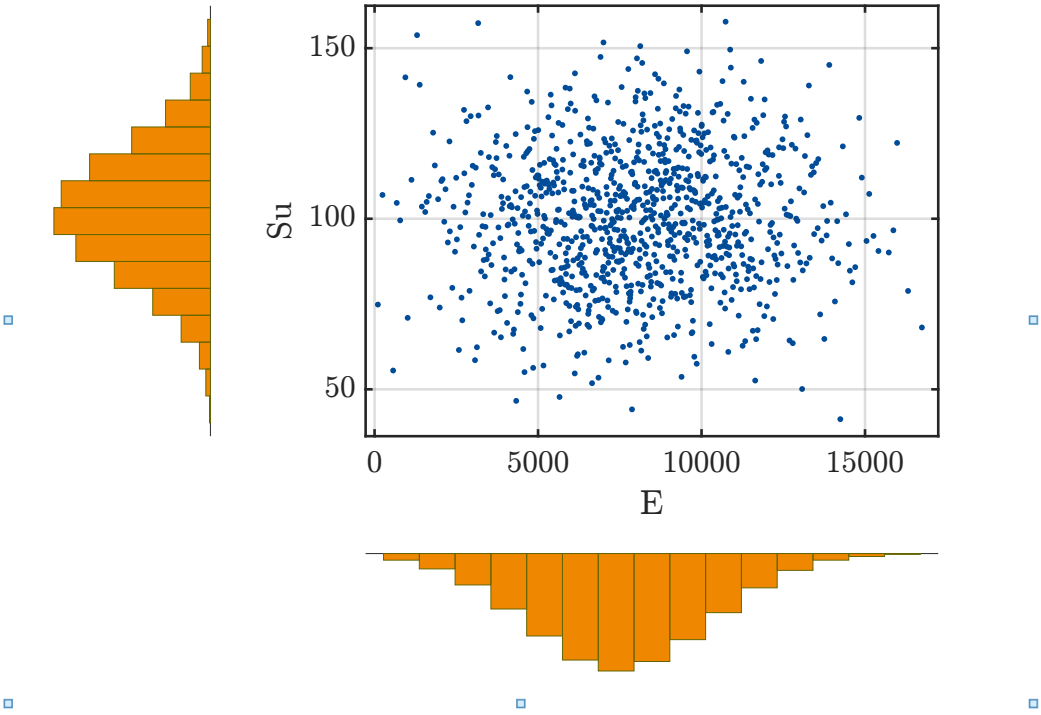

Figure 3: Joint and marginalized distribution of two model parameters.

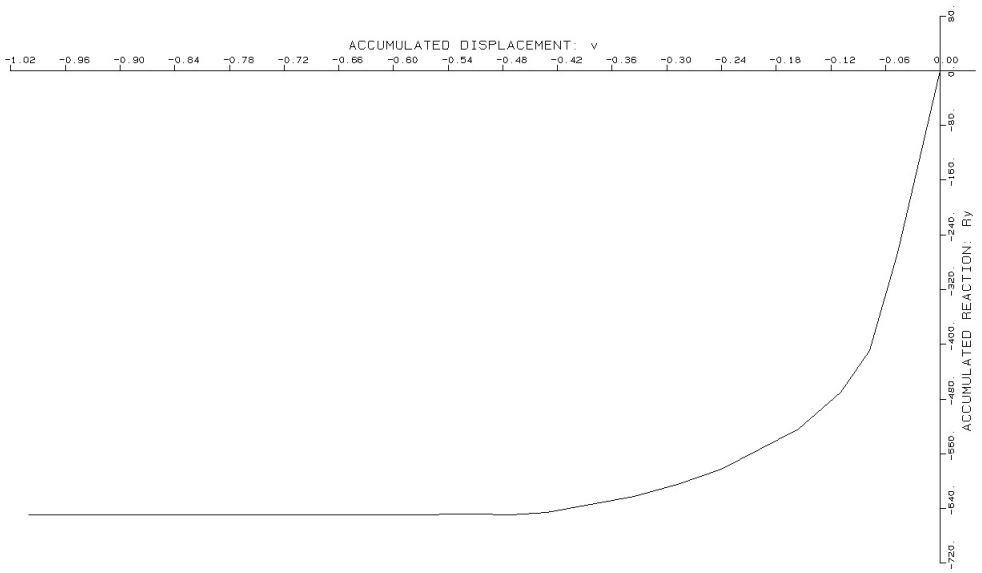

Figure 4: Typical load-displacement curve

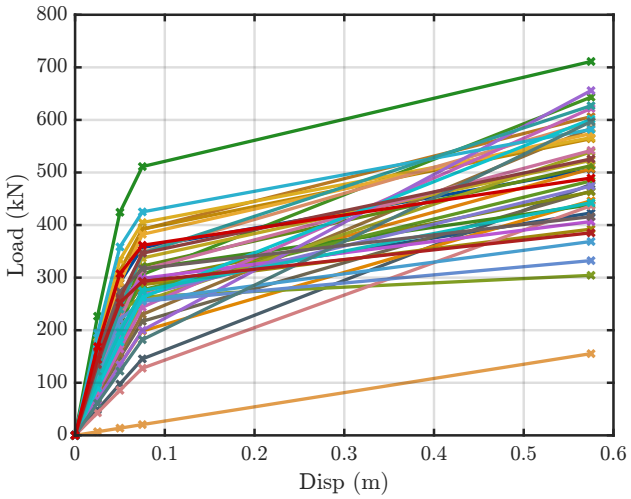

Figure 5: Range of load-displacement curves from the forward model

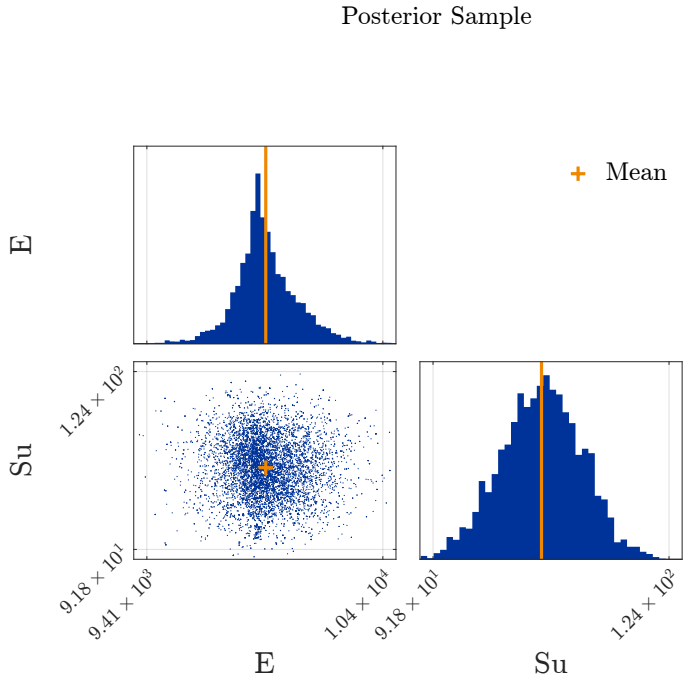

Figure 6: Posterior distribution following Bayesian analysis at the end of stage 1

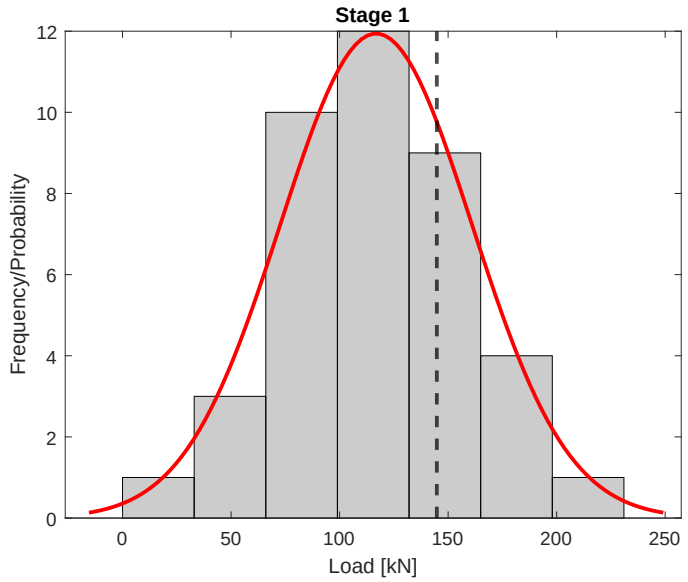

Figure 7: Distribution of forward model results at the end of Stage 1 and $\mathcal{Y}_1$

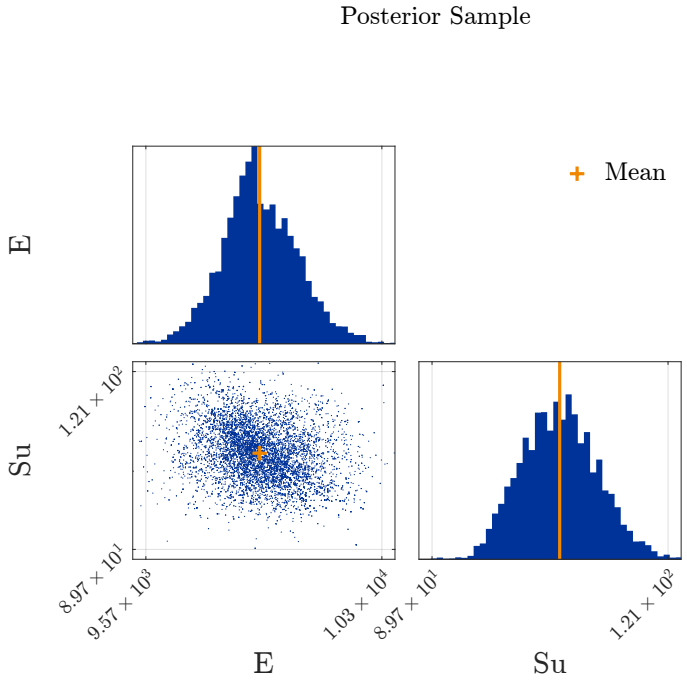

Figure 8: Posterior distribution following Bayesian analysis at the end of stage 2

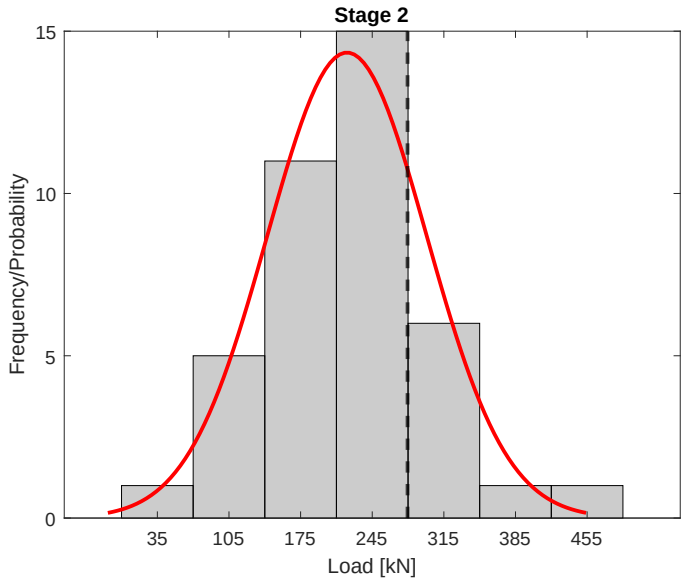

Figure 9: Distribution of forward model results at the end of Stage 2 and $\mathcal{Y}_2$

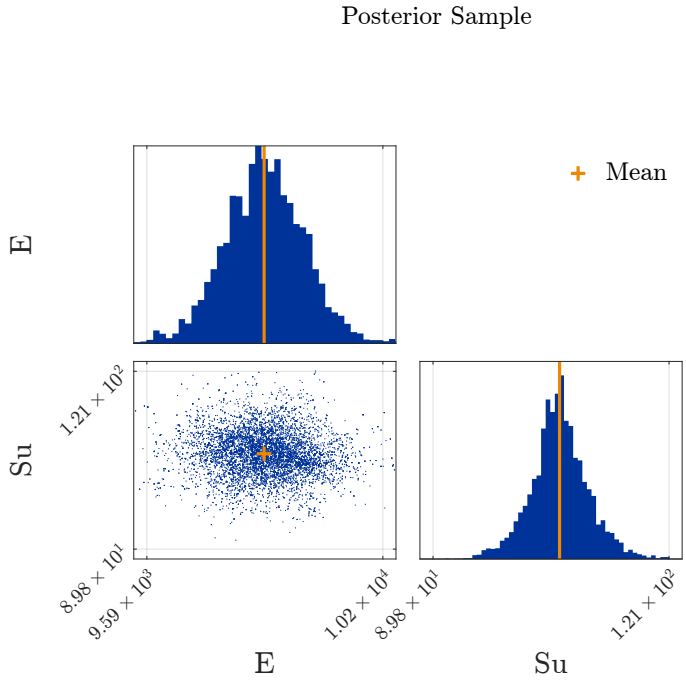

Figure 10: Posterior distribution following Bayesian analysis at the end of stage 3

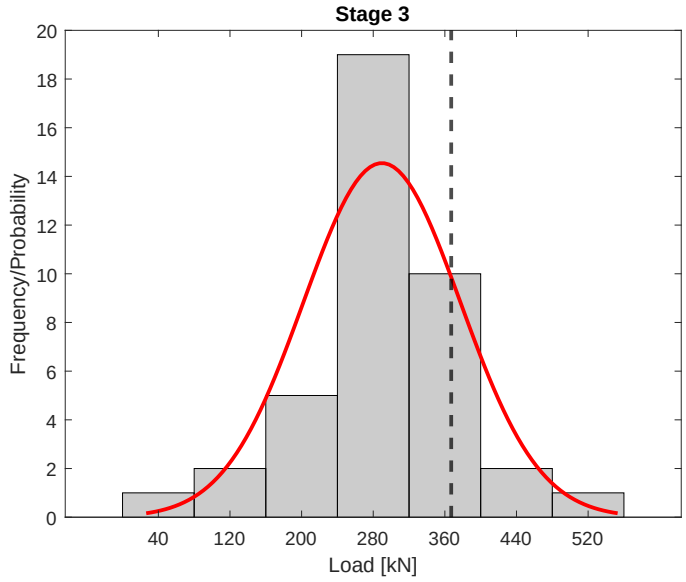

Figure 11: Distribution of forward model results at the end of Stage 3 and $\mathcal{Y}_3$

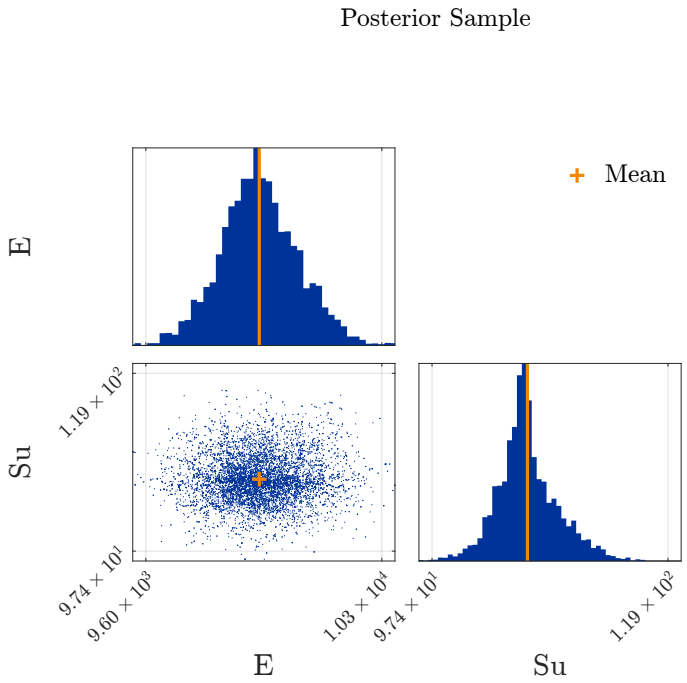

Figure 12: Posterior distribution following Bayesian analysis at the end of stage 4

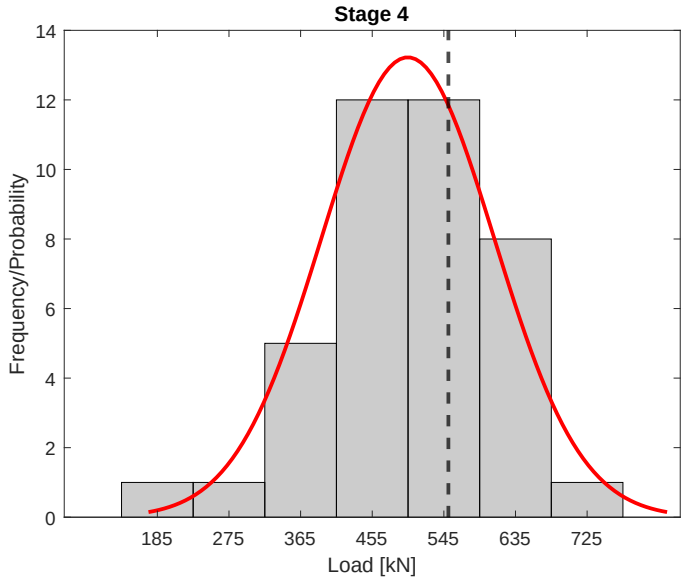

Figure 13: Distribution of forward model results at the end of Stage 4 and $\mathcal{Y}_4$

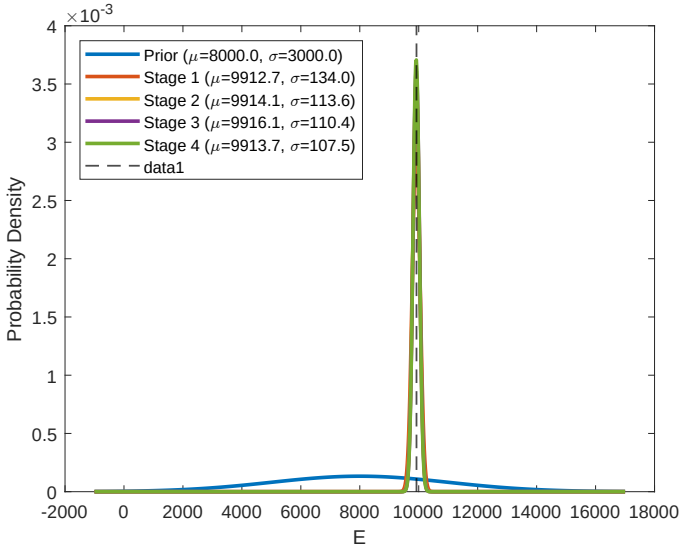

Figure 14: Bayesian inference of E with stage number

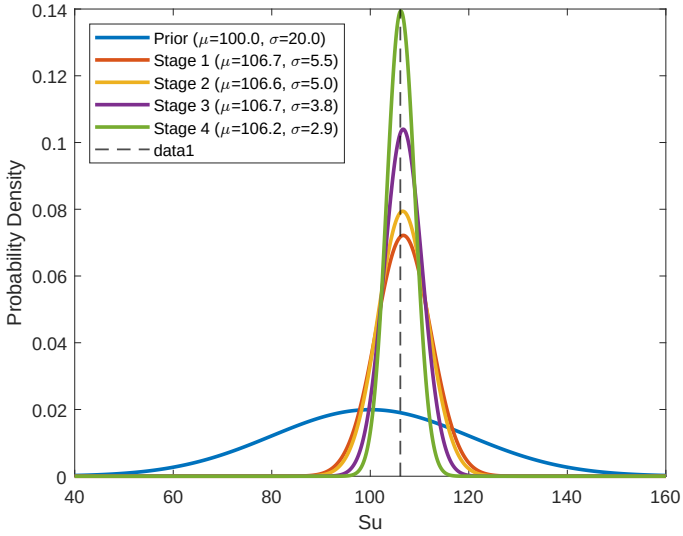

Figure 15: Bayesian inference of s_u with stage number